Sorption and Redox Reactions of As(III) and As(V) within Secondary Mineral Coatings on Aquifer Sediment Grains

David M. Singer[*1], *Patricia M. Fox*[1], *Hua Guo*[2], *Matthew A. Marcus*[3], *James A. Davis*[1]

1. Earth Sciences Division, Lawrence Berkeley National Laboratory

2. Materials Sciences Division, Lawrence Berkeley National Laboratory

3. Advanced Light Source, Lawrence Berkeley National Laboratory

*Corresponding author: dsinger4@kent.edu

* Current address: Department of Geology, Kent State University

Submitted to Environmental Science & Technology 6/21/13

Revised and resubmitted 08/20/13

Supporting Information

Experimental setup of synchrotron x-ray microprobe analysis

The synchrotron x-ray beam size used for the μ-XRF images was 2 μm x 2 μm (APS and SSRL) and 3 μm x 3 μm (ALS) at full width half-maximum using a Pt-coated Kirkpatrick-Baez (K-B) focusing optics system (XRadia). X-ray fluorescence data was collected using a single-element (SSRL) and four-element (APS) Si Vortex Detector (SSI) and seven-element Ge solid-state fluorescence detector (XIA) (ALS). Monochromatic x-rays were selected using a water cooled Si(111) $\varphi = 90$ double crystal monochromator. All data were collected at 1 μm pixel size and 50 ms dwell time per point. The x-ray energy was calibrated to the maximum of the first derivative of a sodium arsenate, As(V), sample spectrum and set at 11869.7 eV. Element maps were collected for the following major and minor/trace elements: As, Ca, Fe, K, Mn, S, Si, Sr, Ti, and Zn. Fluorescence maps were analyzed using the Microanalysis Toolkit.[1] Quantitative determination of As(V) and As(III) at selected locations within the thin sections was accomplished using As K-edge micro-X-ray absorption near-edge structure (μ-XANES) spectroscopy (SSRL); scans were collected from 200 eV below to 300 eV above the As K-edge. Linear combination XANES spectral fitting was performed using SIXPACK[2] to determine the proportion of As(V) to As(III) while minimizing reduced chi square values. Sodium arsenite and sodium arsenate were used as As(III) and As(V) standards for both micro-XANES spectroscopy and As redox mapping, respectively. Arsenic redox mapping (SSRL), following previous methods[3, 4] was performed by collecting maps at 11860 eV, 11872 keV, 11875 keV, and 11880 keV to determine the distribution of As(III) and As(V), and below the Fe K-edge (at 7 keV) to differentiate Mn and Fe spatial distribution. Based on the three As maps, the spatial distribution of As(III), As(V) and total As was based on doing a linear combination fit to the intensity of each pixel as a function of energy. For data from all beamlines, fluorescence counts were normalized to the measured intensity of the incident energy of the x-ray beam (I_0) for each energy map across each line; I_0 did not change (within 1 %) over each map area and for each energy.

For data collected at beamline 10.3.2 at the Advanced Light Source (SI Figure 10), arsenic maps were collected at 11835 eV, 11870 eV, 11873.6 eV, and 11902 eV. Manganese maps were collected at 6530 eV, 6544 eV, 6547 eV, 6552.7 eV, 6555.8 eV, and 6670 eV. Total Fe distribution was collected at 13000 eV. XMP data were acquired with procedures similar to those described in Marcus et al. (2010).[5] Briefly, Mn-bearing reference standards used for the redox mapping included an aqueous $Mn(II)SO_4$ solution, manganite [Mn(III)O(OH)], and ramsdellite [$Mn(IV)O_2$].[6] Additional Mn-bearing references used for comparison were Mn(II) sorbed on fungal biomass and a Mn(IV)-phyllomangate. Redox maps were created by doing a principle component analysis of each pixel in the image based on the six energy values the maps were collected.

Although we did not determine if the EPO-TEK 301-2FL resin reacted with As in the sample and potentially changed the As speciation within the epoxy-embedded samples, previous work using the same resin, similar As concentrations and media, and beamline experimental setup has shown that the resin does not react with or impact the As oxidation state.[7, 8] Further, it is reasonable to assume that this lack of reactivity is true for other redox sensitive elements and compounds.[9, 10]

SI Table 1: R23AW-SAND composite surface area, determined by 10-point N_2-BET analysis (QuantaChrome Autosorb-1-MP gas sorption analyzer). The average surface area is 0.32 ± 0.047 m^2/g.

Replicate	**C parameter**	**Surface Area (m^2/g)**
1	287.55	0.36
2	342.93	0.34
3	323.78	0.27

SI Table 2: The R23AW-SAND composite bulk composition was determined by total digestion. Samples were weighed out in PFA digestion liners on a balance with 0.1 mg resolution. The following were then added to the liners: 3 mL hydrofluoric acid (HF), 2 mL nitric acid (HNO_3), 1 mL hydrochloric acid (HCl), and 2 mL de-ionized water. All acids where ultra-high purity grade (BDH Aristar Ultra).Liners were capped, mounted in pressure vessels and put into microwave reaction system (Anton PaarMultiwave 3000 with rotor 8SXF100) and digested at ~260*C and <1700 psi. This method used a maximum power of 1400W with 10 minute ramp time and 30 minute hold (digestion) time.

Upon digestion and cooling to ambient temperature, samples were transferred to a 10 mL PFA volumetric flask and diluted using de-ionized water. Each PFA flask was calibrated before use to minimize volume error. An aliquot from each digested sample was then diluted 50 times, spiked with internal standard (Li-6, Ga-71, Rh-103, Tm-169) and analyzed using a Perkin Elmer SCIEX Elan DRC II using a quantitative method.

Total extractable As concentrations for the cores which were used to create this sample are 2-4 nmol/g (0.15-0.30 ppm) and As is relatively uniformly distributed.[11] This means that for the 0.5 hr As(III)-treated sample, ~50% of As is native and 50% from added As. For the 24-hr As(III)-treated sample it's about 95% added As and 5% native.

Element	Concentration (μg/g)	Uncertainty (μg/g)
Na	2,200	353
Mg	343	35
Al	8,970	633
Si	497,000	34,100
K	5,970	427
V	7.28	0.44
Cr	3.31	0.26
Mn	29.6	1.5
Ca	352	21
Fe	3,600	229
Ti	531	31
Sr	16.70	2.35
Ba	103	6
Ce	5.53	0.78
Pb	4.39	0.37
Th	0.435	0.068
U	0.62	0.05

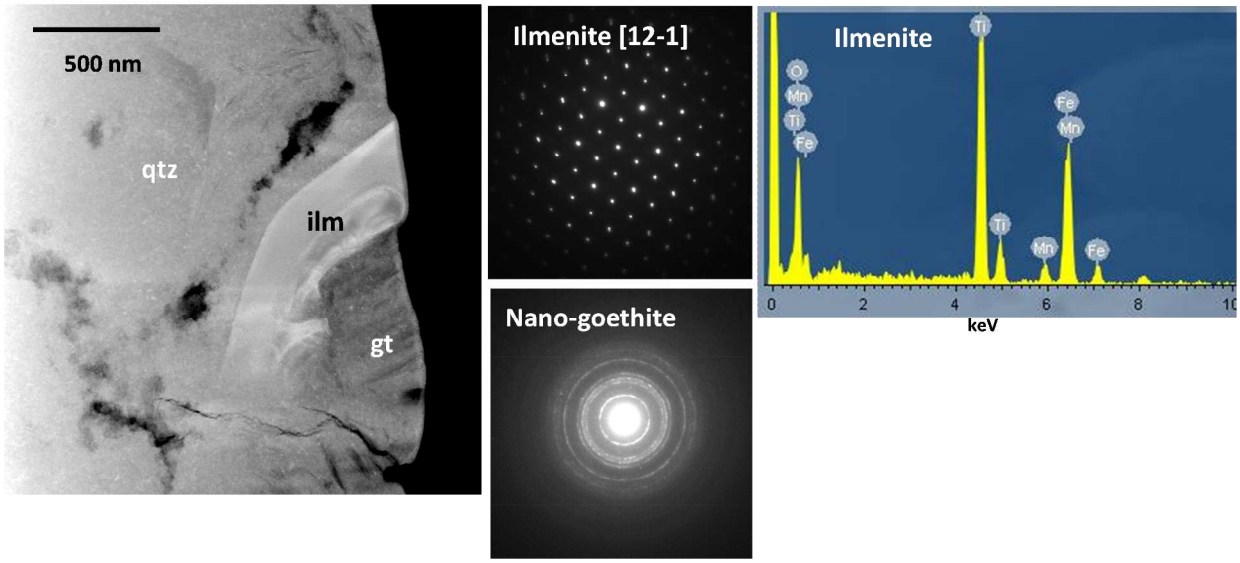

SI FIG 1: Additional TEM dark field image of a FIB-extracted grain coating (right), electron diffraction patterns (center) and an EDS spectrum highlighting the presence of both nanoparticulate goethite (gt) and ilmenite (ilm) in the mineral coatings. This sample was exposed to As(III) for 30 minutes.

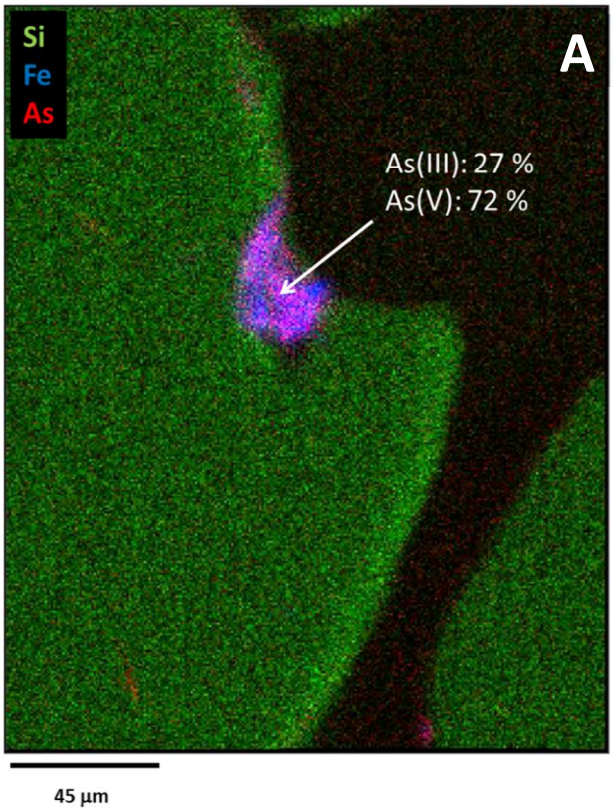

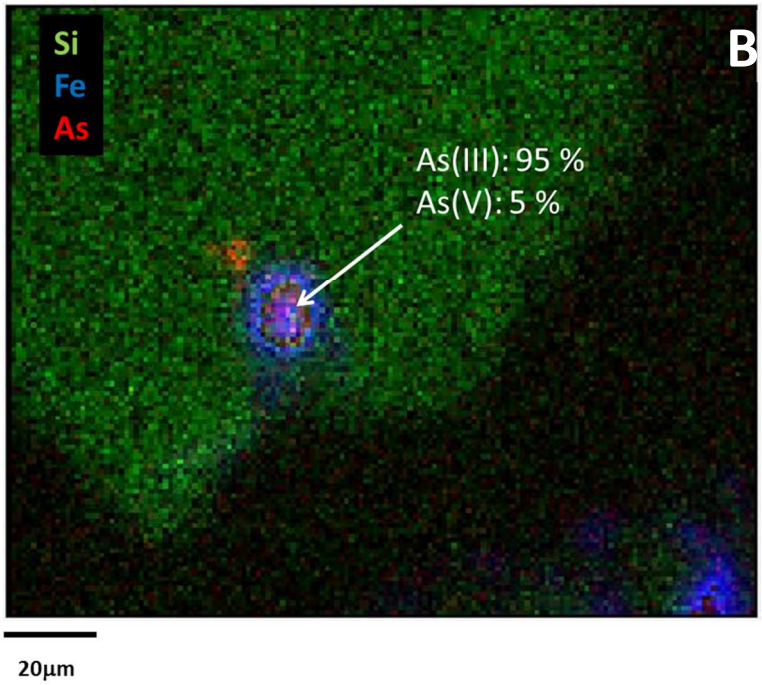

SI Figure 2. Additional XMP maps (SSRL) of two quartz grain edges in a polished thin section, showing Fe and As fluorescence and As redox speciation. The arrow points to the approximate location where micro-XANES spectra were collected. This sample was exposed to As(III) for 30 minutes.

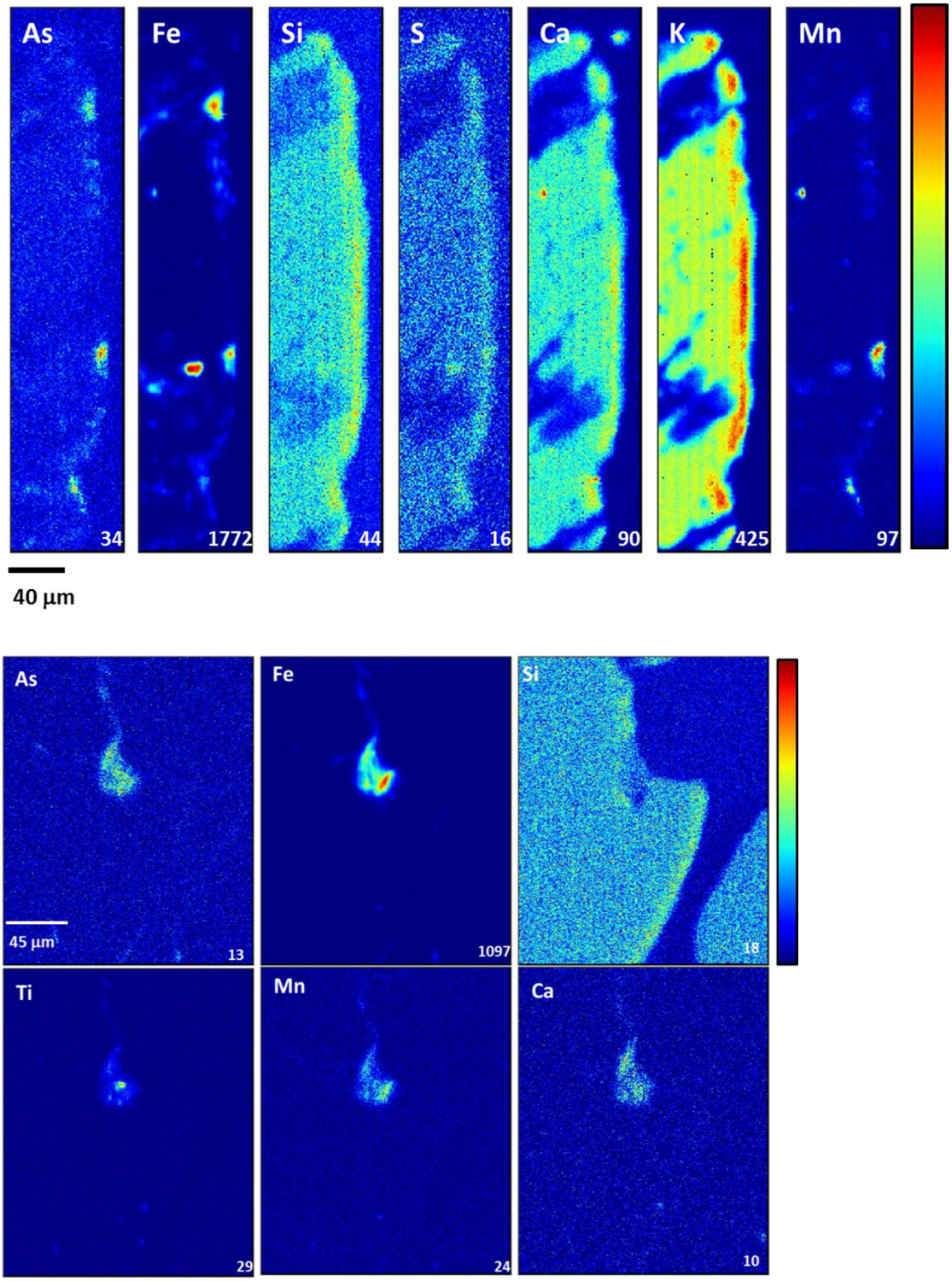

SI Figure 3. Additional XMP element maps (SSRL) of R23AW-SAND after exposure to $As(III)_{aq}$ for 30 minutes. The maps show the edges of two quartz grains in polished thin sections. The numbers in the lower right corner of each map are the maximum fluorescence count value corresponding to the color legends at right; minimum values are zero counts.

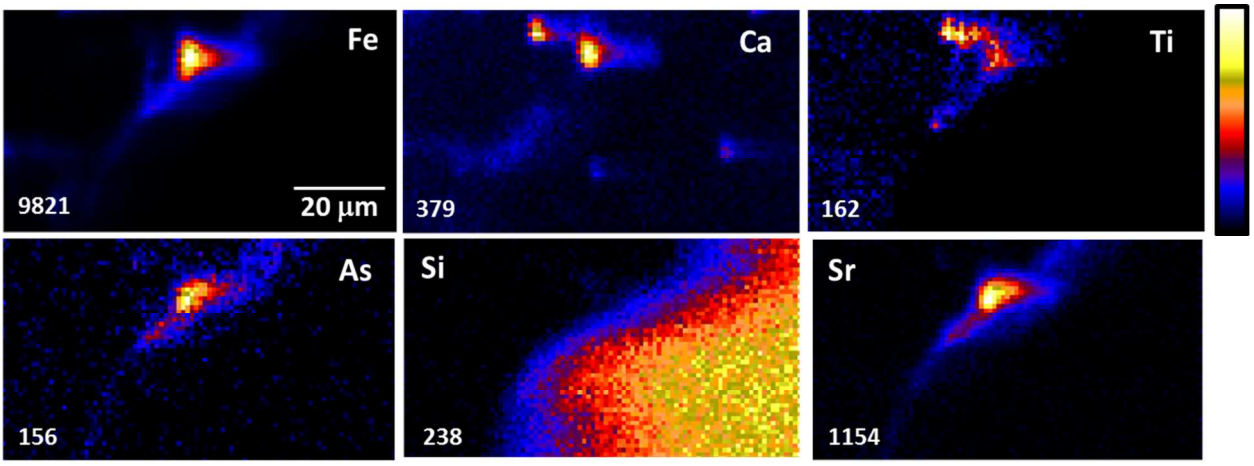

SI Figure 4. Additional XMP element maps (APS) of R23AW-SAND after exposure to $As(III)_{aq}$ for 2 hours. The maps show the edge of one quartz grain in a polished thin section. The numbers in the lower left corner of each map are the maximum fluorescence count value corresponding to the color legends at right; minimum values are zero counts. XMP data were acquired with procedures similar to those described in Newville et al. (1999).[12]

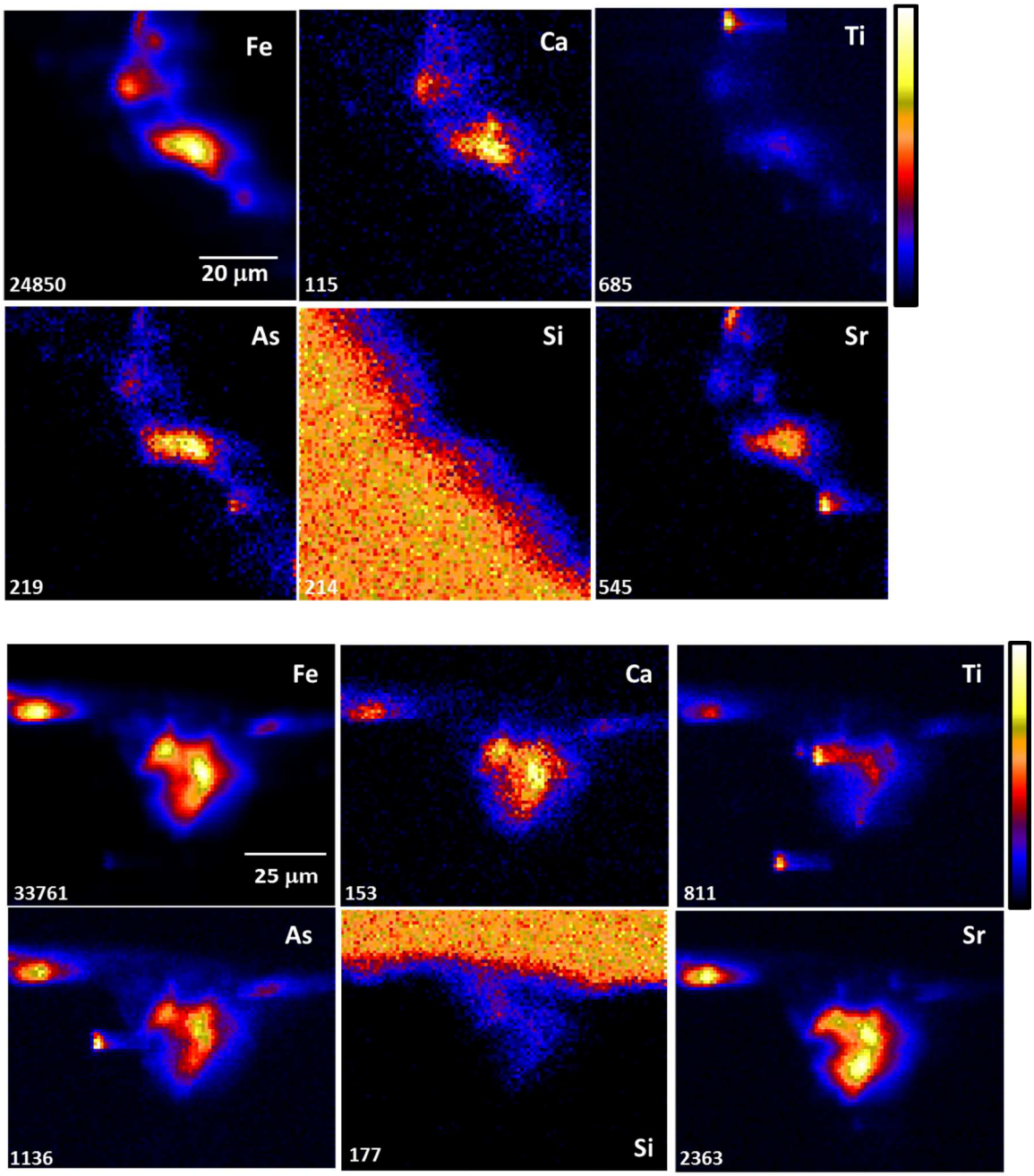

SI Figure 5. Additional XMP element maps (APS) of R23AW-SAND after exposure to $As(III)_{aq}$ for 24 hours. The maps show the edges of two quartz grains in polished thin sections. The numbers in the lower left corner of each map are the maximum fluorescence count value corresponding to the color legends at right; minimum values are zero counts.

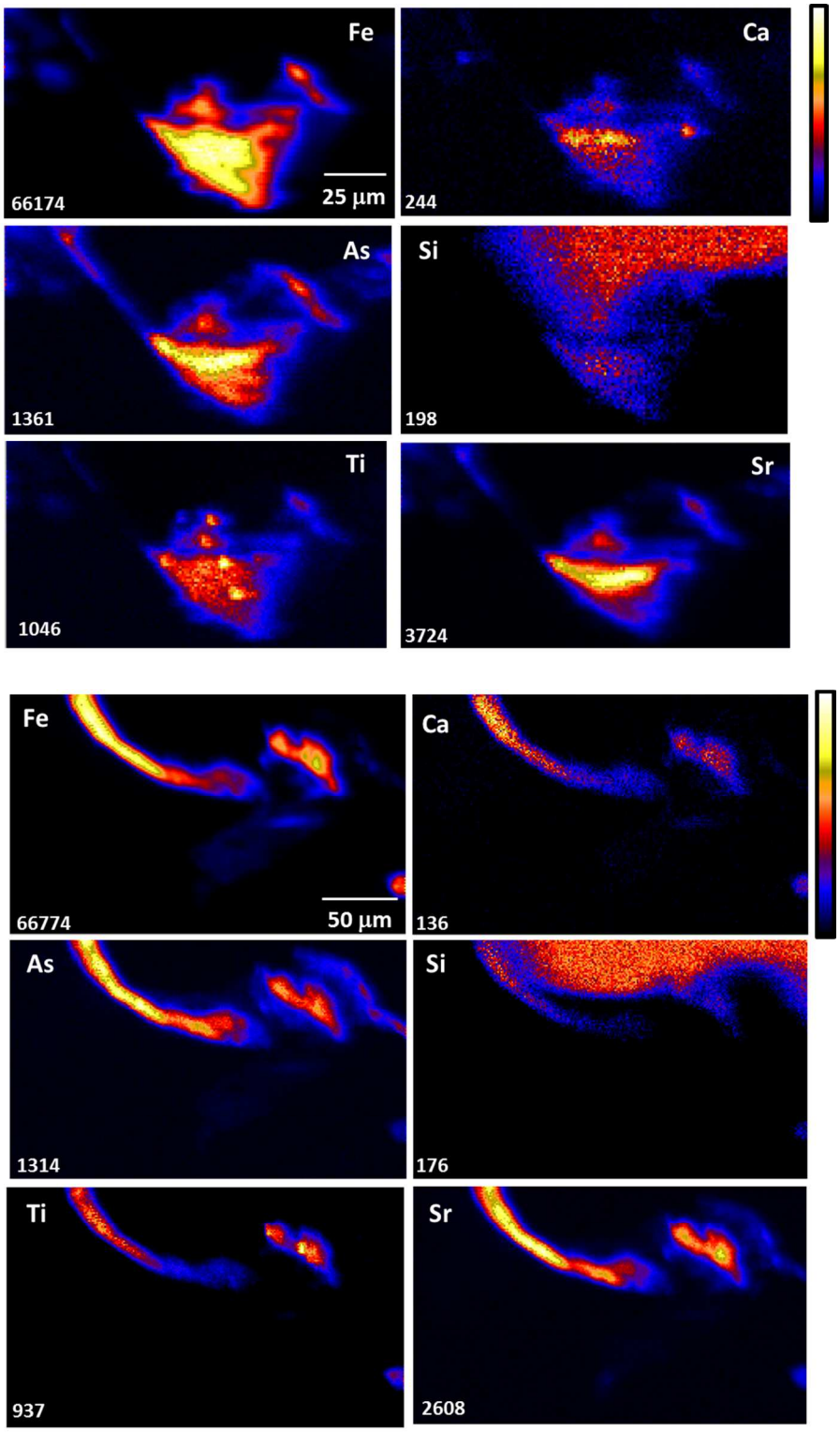

SI Figure 6. Additional XMP element maps (APS) of R23AW-SAND after exposure to $As(V)_{aq}$ for 24 hours. The maps show the edges of two quartz grains in polished thin sections. The numbers in the lower left corner of each map are the maximum fluorescence count value corresponding to the color legends at right; minimum values are zero counts.

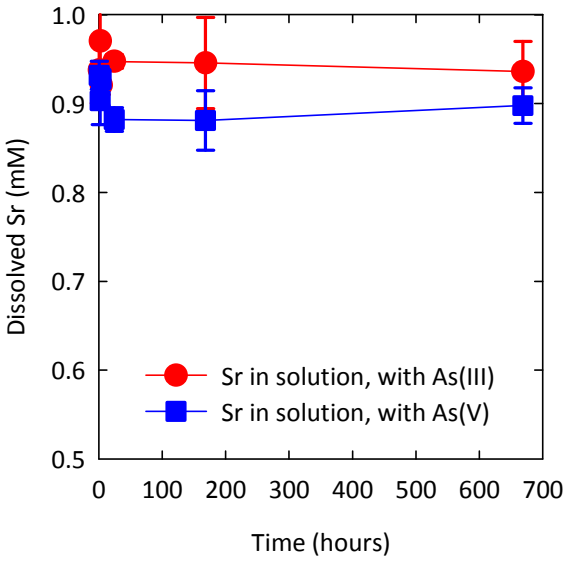

SI Figure 7. Strontium batch sorption results versus time showing dissolved Sr remaining in solution in As(III)- and As(V)-bearing solutions; error bars represent two standard deviation values.

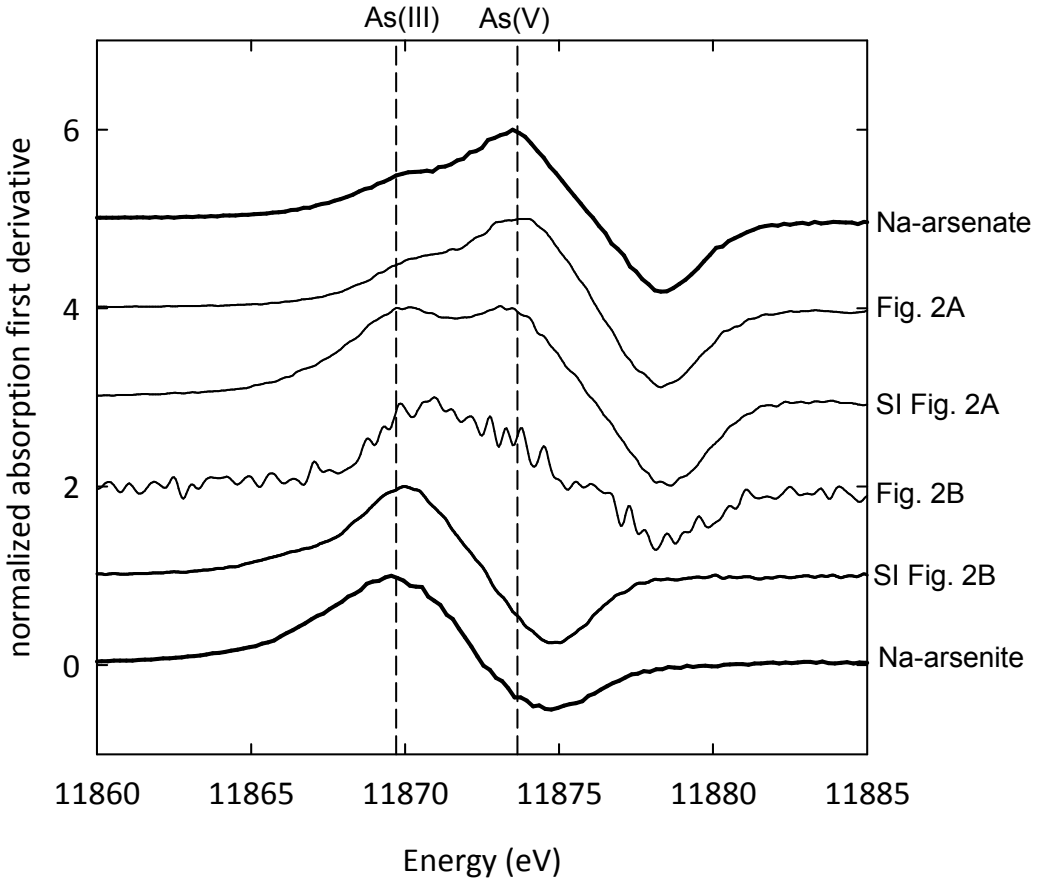

SI Figure 8: First derivative micro-XANES spectra. Location labels refer to the approximate location of where the arrows point in the respective figures. Sodium arsenite and sodium arsenate were used as As(III) and As(V) standards, respectively.

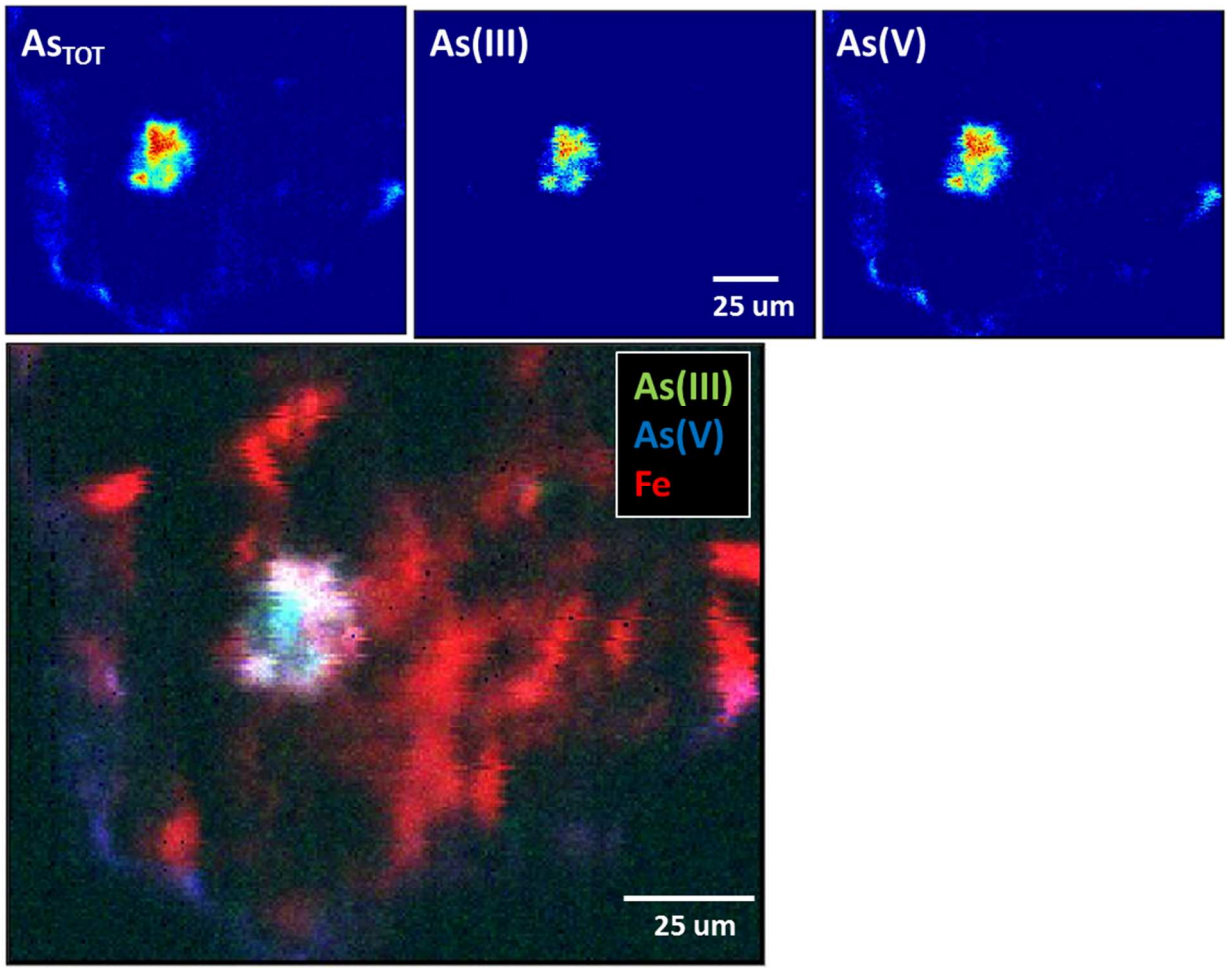

SI Figure 9. Arsenic redox XMP images based on maps collected at 11860 eV, 11872 eV, 11875 eV, and 11880 eV to determine the distribution of As(III) and As(V) and at 15000 eV for Fe spatial distribution. The maps show the edges and interior of a quartz grain in a polished thin section. This sample was exposed to As(III) for 30 minutes. The "whitish" area near the center is an artifact of overlapping distributions of As(III), As(V), and Fe near their maximum fluorescence counts in this image.

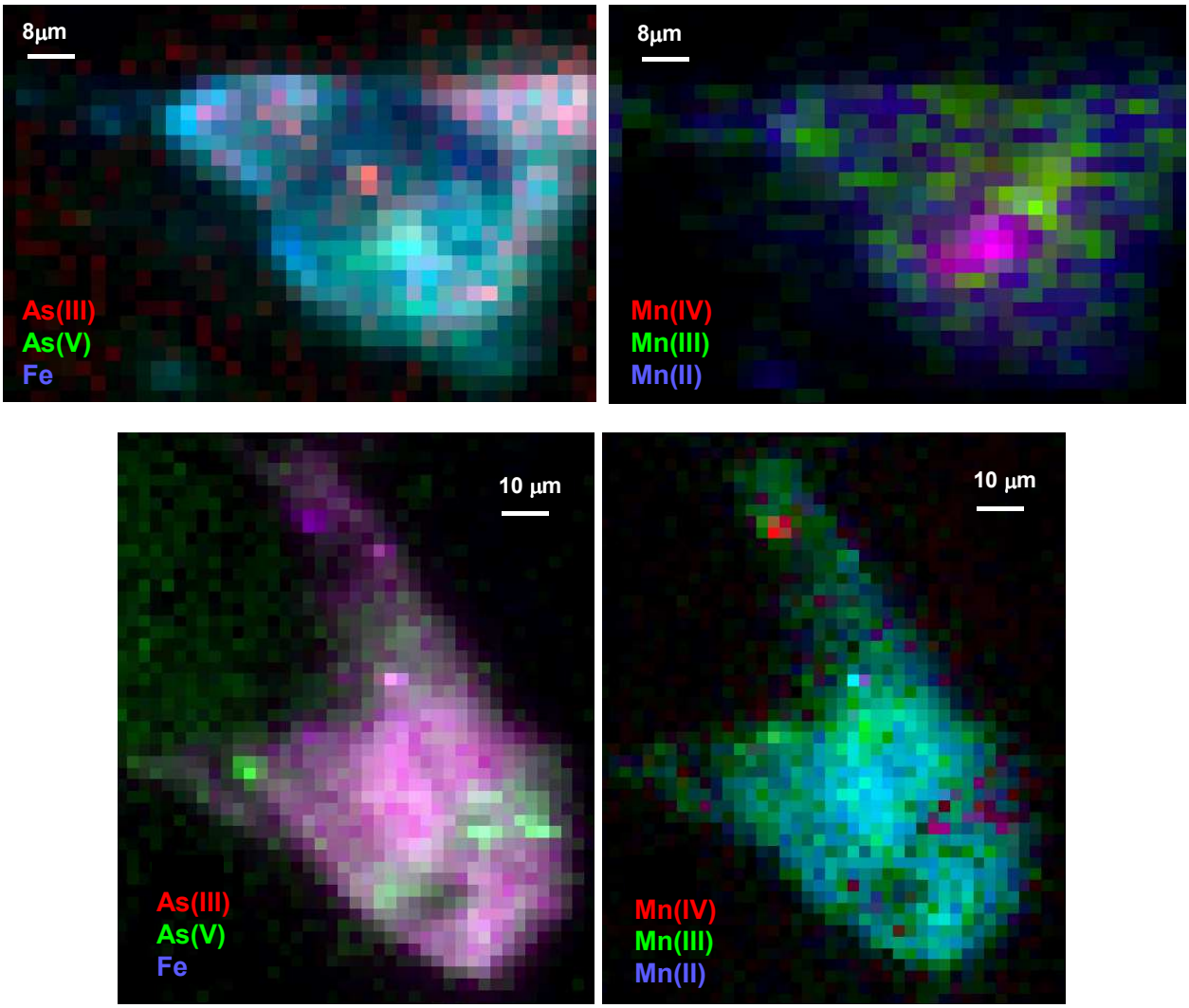

SI Figure 10. Arsenic (left) and manganese (right) redox maps and total Fe spatial distribution collected at the Advanced Light Source, beamline 10.3.2, on the edges of two grains of a polished thin section. This sample was exposed to As(III) for 30 minutes.

References

1. Webb, S. M., The MicroAnalysis Toolkit: X-ray Fluorescence Image Processing Software. *AIP Conference Proceedings* **2011,** *1365*, 196-199.
2. Webb, S., SixPACK: a graphical user interface for XAS analysis using IFEFFIT. *Phys. Scr.* **2005,** *T115*, 1011-1014.
3. Masue-Slowey, Y.; Kocar, B. D.; Bea Jofré, S. A. s.; Mayer, K. U.; Fendorf, S., Transport Implications Resulting from Internal Redistribution of Arsenic and Iron within Constructed Soil Aggregates. *Environ. Sci. Technol.* **2010,** *45*, (2), 582-588.
4. Ying, S. C.; Masue-Slowey, Y.; Kocar, B. D.; Griffis, S. D.; Webb, S.; Marcus, M. A.; Francis, C. A.; Fendorf, S., Distributed microbially- and chemically-mediated redox processes controlling arsenic dynamics within Mn-/Fe-oxide constructed aggregates. *Geochim. Cosmochim. Acta* **2013,** *104*, (0), 29-41.
5. Marcus, M. A., X-ray photon-in/photon-out methods for chemical imaging. *"TrAC, Trends Anal. Chem. "* **2010,** *29*, (6), 508-517.
6. Manceau, A.; Marcus, M. A.; Grangeon, S., Determination of Mn valence states in mixed-valent manganates by XANES spectroscopy. *Am. Mineral.* **2012,** *97*, (5-6), 816-827.
7. Arai, Y.; Lanzirotti, A.; Sutton, S.; Davis, J. A.; Sparks, D. L., Arsenic Speciation and Reactivity in Poultry Litter. *Environ. Sci. Technol.* **2003,** *37*, (18), 4083-4090.
8. Seyfferth, A. L.; Webb, S. M.; Andrews, J. C.; Fendorf, S., Defining the distribution of arsenic species and plant nutrients in rice (Oryza sativa L.) from the root to the grain. *Geochim. Cosmochim. Acta* **2011,** *75*, (21), 6655-6671.
9. Strawn, D.; Doner, H.; Zavarin, M.; McHugo, S., Microscale investigation into the geochemistry of arsenic, selenium, and iron in soil developed in pyritic shale materials. *Geoderma* **2002,** *108*, (3–4), 237-257.
10. Zhuang, Y.; Ahn, S.; Seyfferth, A. L.; Masue-Slowey, Y.; Fendorf, S.; Luthy, R. G., Dehalogenation of Polybrominated Diphenyl Ethers and Polychlorinated Biphenyl by Bimetallic, Impregnated, and Nanoscale Zerovalent Iron. *Environ. Sci. Technol.* **2011,** *45*, (11), 4896-4903.
11. Kent, D.; Fox, P., The influence of groundwater chemistry on arsenic concentrations and speciation in a quartz sand and gravel aquifer. *Geochem. Trans.* **2004,** *5*, (1), 1-12.
12. Newville, M.; Sutton, S. R.; Rivers, M. L.; Eng, P., Micro-beam x-ray absorption and fluorescence spectroscopies at GSECARS: APS beamline 13ID. *J. Synchrotron Rad.* **1999,** *6*, (3), 353-355.